Table III. Redox Properties of Blue Copper Centers

	plasto-cyanin[a]	azurin	stella-cyanin	laccase fungal	laccase tree
reduction potential[b]	360[c]	308[c]	191[c]	785[d]	394[d]
enthalpy of reduction[e]	-13.7	-16.6	-10.3	-22.1	

[a] Bean plastocyanin. [b] mV as NHE. [c] Reference 15. [d] Reference 19. [e] kcal/mol; ref 15.

systems studied, although interpretation of this difference, and the unusual properties of the copper hyperfine tensor of stellacyanin, as well, must await identification of the full set of ligands for the Cu(II) in this protein.[37]

A particularly interesting feature of these considerations is the emergence of a correlation between the reduction potentials of the single-site type 1 Cu(II) centers (Table III) and the bonding within a center, as reflected in the ligand ENDOR parameters (Table I): Reduction potentials decrease directly with decreasing hyperfine couplings to each of the two coordinating ^{14}N and with decreasing coupling to the cysteine protons.

The ligand hyperfine couplings, most especially the nitrogenous ligands, should vary directly with the strength of the bonding to (or ligand field at) the copper(II), which thus decreases in the order, plastocyanins > azurin > stellacyanin. Surprisingly, this is also the order of decreasing reduction potentials; in addition, stellacyanin also has the least exothermic enthalpy of reduction. We conclude from this that a variation in coordination environment that reduces the binding to Cu(II) must be accompanied by a similar but greater effect on the Cu(I) state. For example, the low reduction potential and small ligand hyperfine couplings of stellacyanin, as compared to plastocyanin, together indicate that a decreased stabilization of Cu(II) in stellacyanin is accompanied by an even greater destabilization of the Cu(I). In short, these results suggest that fine tuning of the reduction potential of a single-site type 1 Cu center is primarily achieved by altering the properties of the reduced, Cu(I), state.

In contrast, the blue copper site of fungal laccase has a rather low value for its larger ^{14}N coupling but the highest reduction potential and the most exothermic reduction enthalpy of the centers considered. In this case any weakening of the Cu(II)-N(His) interactions must be accompanied by strengthening in the Cu(I) state. This interpretation focusses attention on the inference, drawn from the proton ENDOR results, that the laccase coordination geometry increases Cu-S π-bonding. Since this is expected to be more influential in stabilizing Cu(I) than Cu(II), it may be that π-bonding is the factor that determines the reduction potential of the laccases. In support of this possibility, the proton couplings of the type 1 Cu(II) in tree laccase are less than those in the fungal protein, and the reduction potential is also less, although it is still greater than for any of the single-site proteins.

Acknowledgment. B.M.H. thanks Prof. Allen Hill for helpful discussions regarding H-D exchange in azurin. We thank Dr. Mitsuo Murata for supplying a sample of highly purified poplar plastocyanin. This work has been supported by National Institutes of Health Grants HL 13531 (B.M.H.), AM 19038 (H.B.G.), and HL 13399 (J.P.) and by Grants from the Australian Research Grants Committee (H.C.F.) and Swedish National Research Council and European Molecular Biology Organization (B.R.).

Registry No. Cu, 7440-50-8; laccase, 80498-15-3.

^1H NMR Nuclear Overhauser Enhancement and Paramagnetic Relaxation Determination of Peak Assignment and the Orientation of Ile-99 FG5 in Metcyanomyoglobin

S. Ramaprasad, Robert D. Johnson, and Gerd N. La Mar*

Contribution from the Department of Chemistry, University of California, Davis, California 95616. *Received February 27, 1984*

Abstract: The interproton nuclear Overhauser effect (NOE) and paramagnetic dipolar relaxation rates for hyperfine-shifted resonances in the upfield portions of the 360-MHz NMR spectrum of sperm whale metcyanomyoglobin has led to the location and assignment of all six nonequivalent proton signals of an isoleucine in the heme pocket. NOEs between previously assigned heme methyls and Ile protons establish it as Ile-99 (FG5). Differential dipolar relaxation rates indicate that the orientation of Ile-99 is essentially the same as in single crystals. The time dependence of the interproton NOE for the γ-geminal protons indicates limited internal mobility for this side chain. The nature of the direction and relative magnitudes of the necessarily dipolar origin of the Ile-99 hyperfine shifts clearly demonstrate that the heme iron exhibits substantial rhombic as well as axial magnetic anisotropy and that the effective in-plane magnetic axes are not the same as observed in single crystals at cryogenic temperature.

It has been long recognized that van der Waals interactions between the folded polypeptide side chains and the heme play a crucial control function in hemoproteins.[1] Such interactions can involve imposing steric strain on the porphyrin skeleton,[2] modulation of the iron reactivity via π-π interaction with aromatic side chains,[3] steric blocking at the distal binding site,[4] and/or electronic, steric, and hydrogen-bonding interaction with a bound ligand.[5,6] While high-resolution X-ray diffraction studies have provided a wealth of structural details of both myoglobin[7,8] and hemoglobin[9,10] in single crystals, it has also become obvious that only through

* Present address: Department of Chemistry, University of California, Davis, CA 95616.

(1) Antonini, E.; Brunori, M. "Hemoglobin and Myoglobin in their Reactions with Ligands"; American Elsevier: New York, 1971; Chapter 4, p 13.
(2) Gelin, B. R.; Karplus, M. *Proc. Natl. Acad. Sci. U.S.A.* **1977**, *74*, 801.
(3) Rousseau, D. L.; Shelnutt, J. A.; Ondrias, M. R.; Friedman, J. M.; Henry, E. R.; Simon, S. R. In "Hemoglobin and Oxygen Binding"; Ho, C., Ed.; Elsevier-Biomedical: New York, 1982; pp 223-229.
(4) Case, D. A.; Karplus, M. *J. Mol. Biol.* **1979**, *132*, 343.
(5) Satterlee, J. D.; Teintze, M.; Richards, J. H. *Biochemistry* **1978**, *17*, 1456.

0002-7863/84/1506-5330$01.50/0

the mobility of side chains can the substrate enter or leave the heme cavity.[4]

Nuclear magnetic resonance has played a key role in providing a detailed picture of the influence of the subtle perturbations of the protein structure on the electronic structure of the heme.[11,12] These investigations rely heavily on the unambiguous assignment of the ^{1}H NMR resonances. While this has been largely accomplished for the resonances of the heme using systematic specific deuteration of all functional groups,[13-15] unambiguous assignment of noncoordinated residues in the heme pocket is much more difficult and requires the development of indirect methods.[16] While the ^{1}H NMR spectrum of metMbCN,[13,17] for example, exhibits numerous hyperfine-shifted signals which do not originate from the heme and therefore must originate from side-chain protons in the immediate vicinity of the iron center, it has not been possible to make even tentative assignments in most cases. The close proximity to the iron of exchangeable protons from the proximal and distal histidyl imidazole has permitted their assignment on the basis of differential paramagnetic relaxation,[18] and it is likely that analysis of such relaxation data must be relied on to provide further progress in this area.

Residues whose ^{1}H NMR properties would be of particular interest are those that interact with the ligand binding site, i.e., histidine E7 and valine E11,[5-10] and the residues that make close contact with the heme, Phe CD1, His FG3, Leu F4, and Ile FG5.[7-10] The last residue, in particular, has been proposed to play a key role in the molecular basis of cooperativity in hemoglobins.[2] The metcyano form of hemoproteins, which is a satisfactory model for the CO-ligated form of Mb and Hb, provides the optimal case for the resolution and identification of the signals from the residues in the heme pocket, because the substantial magnetic anisotropy induces large hyperfine shifts for noncoordinated residues.[11,12] The magnitude of these hyperfine shifts could, in principle, lead to assignment of resonances by using the equation for the necessarily dipolar paramagnetic shift,[19] i.e.,

$$(\Delta H/H) = -D(3\cos^2\theta - 1)r^{-3} + D'\sin^2\theta\cos 2\Omega r^{-3} \quad (1)$$

where $D = [\chi_{zz} - {}^1/_2(\chi_{xx} - \chi_{yy})]/(3N)$, $D' = [\chi_{xx} - \chi_{yy}]/(2H)$, θ is the angle between the Fe–proton vector and the z axis, r is the length of the vector, and Ω is the angle between the projection of r on the xy plane and the x axis. However, a necessity for a tractable analysis is that axial symmetry applies (i.e., $D' = 0$), so that the shift is simply determined by r alone. In a number of models for low-spin ferric hemoprotein, the validity of this assumption has been quantitatively established.[20] In proteins, however, the in-plane anisotropy may be substantial, making analysis of the shift impossible without knowledge of either the in-plane magnetic axes or D and D' in eq 1.

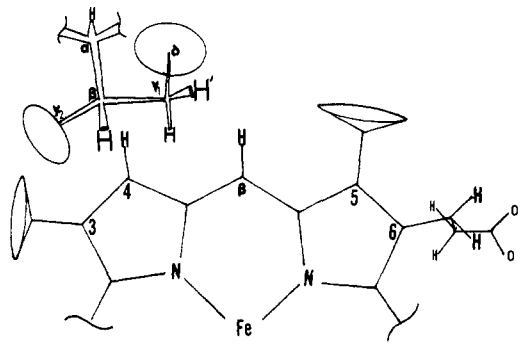

Figure 1. Schematic representation of orientation of Ile-99 (FG5) relative to the heme plane in sperm whale Mb. The position of methyl protons is indicated by the ring representing methyl group rotation.

We have shown that some resonance assignments can be effected on the basis of the r^{-6} dependence of the paramagnetic relaxation by comparison of the relative "non-selective" spin–lattice relaxation rate to that of an assigned and structurally defined proton.[18,21] However, since only distance from the iron can be estimated from relaxation rates, there will always be several candidates for any given resonance unless a spatial relationship among several resonances can be established. The nuclear Overhauser effect, NOE, provides a powerful method for establishing the spatial relationship of both covalently linked and noncovalently linked protons.[22-26] Moreover, if this spatial relationship of two protons is constrained by covalent links, the NOE provides a probe of the internal motion of this interproton vector. There have been very few reports of detecting NOEs in paramagnetic proteins,[27] probably because it is generally assumed that the paramagnetic "leakage" will render the NOE undetectable.[22] The most suitable oxidation/spin state of a hemoprotein for observing NOEs between paramagnetically relaxed protons would be the low-spin ferric form, which invariably exhibits extremely efficient electron spin relaxation and, hence, concomitantly ineffective nuclear relaxation.[11,12]

In a preliminary communication,[28] we have shown that strong NOEs can be observed among a subset of hyperfine-shifted resonances in the upfield portion of the ^{1}H NMR spectra of native metMbCN and deuterohemin-reconstituted metMbCN (2,4-hydrogen rather than vinyls). The five resonances so interconnected involve two methyl groups and at least three single protons. Detection of a NOE between two of these signals and heme 5-CH_3 in both native and deuterohemin-reconstituted metMbCN, as well as the 4-H in the latter compound, clearly establish[28] the identity of the signals as arising from Ile-99 FG5 which lies on the proximal side of the heme[7,8] above pyrroles II and III, as depicted in Figure 1.

We report herein on the dynamics of this NOE buildup which demonstrate its primary origin, assign the individual resonances of Ile-99 FG5, analyze the dipolar relaxation in terms of the average solution orientation of this side chain,[18] and show that the observed dipolar shifts[19] provide clear evidence for the importance of rhombic magnetic anisotropy of the iron.

Experimental Section

Sperm whale myoglobin was purchased from Sigma Chemical Co. (M-0380) and used without further purification. Metcyanomyoglobin

(6) Appleby, C. A.; Bradbury, J. H.; Morris, R. J.; Wittenberg, B. A.; Wittenberg, J. B.; Wright, P. E. *J. Biol. Chem.* **1983**, *258*, 2254.
(7) Takano, T. *J. Mol. Biol.* **1977**, *110*, 537.
(8) Phillips, S. E. V. *J. Mol. Biol.* **1980**, *142*, 531.
(9) Fermi, G. *J. Mol. Biol.* **1975**, *47*, 237.
(10) Perutz, M. F. *Br. Med. Bull.* **1976**, *32*, 195.
(11) Morrow, J. S.; Gurd, F. R. N. *CRC Crit. Rev. Biochem.* **1975**, *3*, 221.
(12) La Mar, G. N. In "Biological Applications of Magnetic Resonance"; Shulman, R. G., Ed.; Academic Press, New York, 1979; pp 305–343.
(13) Mayer, A.; Ogawa, S.; Shulman, R. G.; Yamane, T.; Cavaleiro, J. A. S.; Rocha-Gonsalves, A. M. d'A.; Kenner, G. W.; Smith, K. M. *J. Mol. Biol.* **1974**, *86*, 749.
(14) La Mar, G. N.; Budd, D. L.; Smith, K. M.; Langry, K. C. *J. Am. Chem. Soc.* **1980**, *102*, 1822.
(15) Krishnamoorthi, R. Ph.D. Thesis, University of California, Davis, 1982.
(16) Keller, R. M.; Wüthrich, K. In "Biological Magnetic Resonance"; Berliner, L. J., Reuben, J., Eds.; Plenum Press: New York, 1981; Vol. 3, pp 1–52.
(17) Shulman, R. G.; Wüthrich, K.; Yamane, T.; Antonini, E.; Brunori, M. *Proc. Natl. Acad. Sci. U.S.A.* **1969**, *63*, 623.
(18) Cutnell, J. D.; La Mar, G. N.; Kong, S. B. *J. Am. Chem. Soc.* **1981**, *103*, 3567.
(19) Jesson, J. P. In "NMR of Paramagnetic Molecules"; La Mar, G. N., Horrocks, W. D., Holm, R. H., Eds.; Academic Press: New York, 1973; pp 1–51.
(20) La Mar, G. N.; Viscio, D. B.; Smith, K. M.; Caughey, W. S.; Smith, M. L. *J. Am. Chem. Soc.* **1978**, *100*, 8085.
(21) Kong, S. B.; Cutnell, J. D.; La Mar, G. N. *J. Biol. Chem.* **1983**, *258*, 3843.
(22) Noggle, J. H.; Shirmer, R. E. "The Nuclear Overhauser Effect"; Academic Press: New York, 1971.
(23) Wagner, G.; Wüthrich, K. *J. Magn. Reson.* **1979**, *33*, 675.
(24) Olejniczak, E. T.; Poulsen, F. M.; Dobson, C. M. *J. Am. Chem. Soc.* **1981**, *103*, 6574.
(25) Dobson, C. M.; Olejniczak, E. T.; Poulsen, F. M.; Ratcliff, R. G. *J. Magn. Reson.* **1982**, *48*, 97.
(26) Gordon, S.; Wüthrich, K. *J. Am. Chem. Soc.* **1978**, *100*, 7094.
(27) Trewhella, J.; Wright, P. E.; Appleby, C. A. *Nature (London)* **1980**, *280*, 87.
(28) Johnson, R. D.; Ramaprasad, S.; La Mar, G. N. *J. Am. Chem. Soc.* **1983**, *105*, 7205.

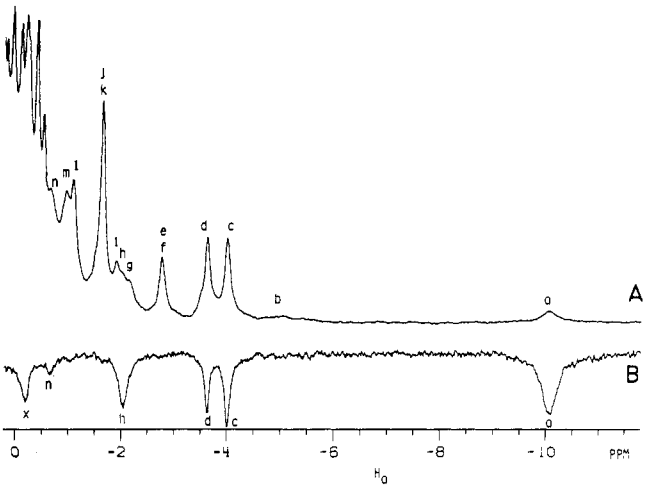

Figure 2. (A) Upfield hyperfine-shifted portion of the 360-MHz ^1H NMR spectrum of sperm whale metMbCN in ^2H_2O, pH 8.6, 20 °C. (B) Difference spectrum obtained upon steady-state saturation of peak a at -10 ppm. The vertical scale is expanded ×5 relative to A.

samples were prepared by adding a 4-fold excess of KCN to 3 mM myoglobin solutions in 0.2 M NaCl in ^2H_2O. The "pH" was adjusted by addition of 0.1 M NaO^2H or 0.1 M ^2HCl; solutions were centrifuged before being transferred to 5-mm NMR tubes. The pH was measured with a Beckman 3550 pH Meter equipped with an Ingold 620 microcombination electrode; pH values were uncorrected for the isotope effect. Chemical shifts are referenced to DSS (2,2-dimethyl-2-silapentane-5-sulfonate) through the residual water resonances.

Proton NMR spectra were recorded on a Nicolet 360-MHz spectrometer, using 8K data points over a 10-KHz band width. Time-dependent NOE spectra were taken using the truncated NOE pulse sequence.[23] Saturation pulse lengths varied from 30 to 300 ms; delays between them were 0.7 s. For a given saturation length, two spectra were recorded in an interleaved fashion, the first with the saturation pulse on the resonance, the second with the saturation pulse off-set by 3000 Hz to provide a reference for the difference spectrum. 1600 scans were collected per spectrum; difference spectra were analyzed by area. NOE experiments were repeated to verify accuracy. T_1 measurements were done using the inversion recovery method with composite inversion pulses[29] and phase alternation;[30] delays between scans was maintained to be $>5T_1$.

Results and Discussion

Assignments Based on NOEs. The upfield portion of the 360-MHz ^1H NMR spectrum of sperm whale metMbCN at 20 °C is illustrated in A of Figure 2. It differs from that previously reported at 25 °C[28,31] in that at this temperature peak h is partially resolved. The whole spectrum at 25 °C has been reported a number of times at various field strengths.[13,17,18] The present field strength and sensitivity allow better discrimination of the individual contributing resonances upfield of the diamagnetic envelope. Above -1 ppm we find resolved under some conditions seven single-proton resonances labeled in sequence in the downfield direction, a, b,and e–i, and four three-proton signals, c, d, j, and k, which can be safely attributed to methyl groups. An additional signal, n, with apparent single-proton intensity is observed only at 20 °C on the rapidly rising shoulder of the diamagnetic envelope. The composition of the spectrum at 20 °C and at alternate temperatures is conveniently visualized in Figure 3 as the Curie plot[19] for resonances a and c–k. Of these 11 resonances, three have been definitely assigned by both deuteration[15] and NOEs,[31] indicating that e and i originate from the 2-vinyl cis and trans H_βs, respectively, while line width consideration and model compounds have attributed the broad, poorly defined peak b to the proximal histidyl imidazole 2-H.[32] The ^1H NMR spectrum of

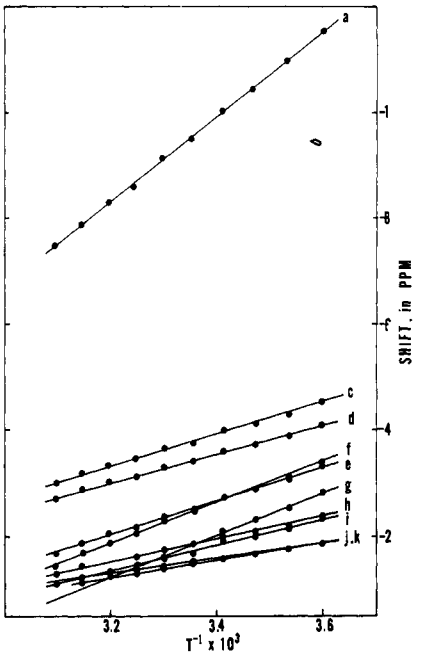

Figure 3. Plot of observed shift vs. reciprocal temperature (Curie plot) for resolved upfield resonances of sperm whale metMbCN in ^2H_2O, pH 8.6; peak designations are the same as in Figure 2.

Table I. Interproton Distances and Observed Nuclear Overhauser Enhancements between Ile-99 and Selected Heme Protons

	saturated peaks		
obsd peaks	Ile-99 a (γ_1-CH)	heme 5-CH_3	deuteroheme 4-H
5-CH_3	5.1–5.7[a] (2%)[b]		6.0–6.1 (0)
a (γ_1-CH)		c	3.60–3.71 (0)
h (γ_1-CH′)	1.77 (47%)	5.30–6.06 (0)	5.12–5.30 (0)
c (δ-CH_3)	2.60–2.62 (13%)	4.39–5.01 (3%)	3.35–3.86 (6%)
d (γ_2-CH_3)	2.77–3.01 (10%)	7.40–7.97 (0)	3.56–3.99 (3%)
n (α-CH)[d]	3.81–3.83 (8%)	7.23–7.67 (0)	5.53–5.88 (0)
x (β-CH)[d]	2.48–2.66 (29%)	7.50–7.99 (0)	5.49–5.96 (0)

[a] Distances (Å) determined from four X-ray structures as described in the Experimental Section. [b] NOE, as percent decrease in signal intensity. [c] Peak too broad and paramagnetic leakage too great to obtain estimate of NOE. [d] NOEs determined assuming single-proton peak intensity for these unresolved resonances.

deuterohemin-reconstituted metMbCN (2,4-hydrogens rather than vinyls) is similar in the upfield region (see Figure 2 in ref 28) except for the missing vinyl peaks and the additional heme 2-H and 4-H signals at -14 and -21 ppm.[33]

As shown previously,[28] saturation of peak a leads to steady-state NOEs as seen in B of Figure 2, with five peaks exhibiting significant intensity in the difference spectrum. The heme 5-CH_3 also shows a small but completely reproducible NOE (see C of Figure 1 in ref 28). Peaks c, d, h, and n are resolved at some temperatures and hence allow quantitative determination of the NOE. The NOE for peak x is estimated on the assumption that it is also a single-proton peak (see below). The resulting steady-state NOEs are listed in Table I.

The buildup of NOEs as a function of irradiation time in a truncated NOE experiment[26] is depicted in Figure 4. The sizeable NOE intensities extrapolate to zero at zero time, indicating that they are primary NOEs for peaks c, d, h, and x.[25] The intensity of n in the difference spectra is too small to determine accurately but is consistent with also being a primary NOE. The observation of the same NOEs in the steady-state and truncated NOE experiments also indicates that spin diffusion is negligible.[25]

The -46% NOE for peak h requires that proton a and h be a geminal pair.[34] The NOE to the heme 5-CH_3 and 4-H (in deuterohemin-metMbCN) already have established[28] that the signals

(29) Freeman, R.; Kempsell, S. P.; Levitt, M. H. *J. Magn. Reson.* **1976**, *38*, 453.
(30) Cutnell, J. D.; Bleich, H. E.; Glasel, S. A. *J. Magn. Reson.* **1976**, *21*, 43.
(31) Ramaprasad, S.; Johnson, R. D.; La Mar, G. N. *J. Am. Chem. Soc.* **1984**, *106*, 3632.
(32) La Mar, G. N.; de Ropp, J. S.; Chacko, V. P.; Satterlee, J. D.; Erman, J. E. *Biochim. Biophys. Acta* **1982**, *708*, 317.
(33) Davis, N. L. Ph.D. Thesis, University of California, Davis, 1982.

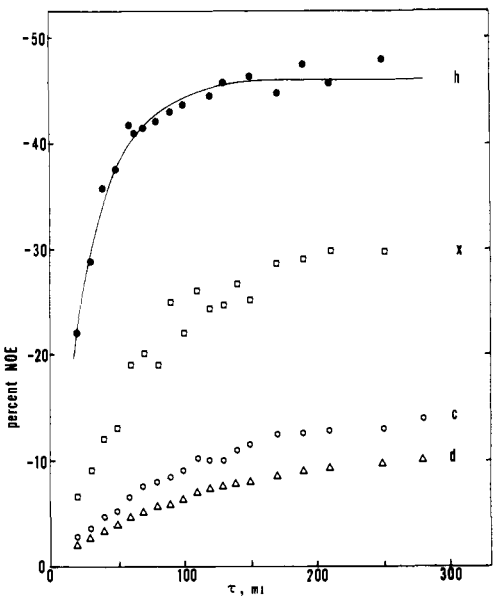

Figure 4. Plot of observed NOEs for resonances c (○), d (△), h (●), and x (□) upon irradiating peak a with rf pulses of variable length, τ (truncated NOE). The solid line represents the least-squares fit of the data points for peak h to eq 3.

Table II. Determination of Iron–Proton Distances from Relative Dipolar Relaxation Times

peak	T_1, ms	r_i,[a] Å	r_i,[b] Å
8-CH_3	144 ± 10	6.10	6.10
a (γ_1-CH)	59 ± 6	4.48–4.72	5.11–5.42
h (γ_1-CH′)	~90 ± 15	5.47–6.00	5.41–5.86
c (δ-CH_3)	193 ± 12	6.47–6.59	6.27–6.55
d (γ_2-CH_3)	204 ± 13	6.35–7.13	6.32–6.61

[a] $r_i = \langle r^3 \rangle^{1/3}$; determined from X-ray coordinates for four different structures as described in the Experimental Section. [b] $r_i = r(CH_3)[T_1(H_i)/T_1(CH_3)]^{1/6}$; r_i estimated assuming $r(CH_3)$ is 6.1 Å.

must arise from Ile-99 FG5. Thus, a and h arise from γ_1-CH_2. The NOE to c but not d upon irradiating 5-CH_3 assigns c to δ-CH_3. The similar NOEs to both c and d in deuterohemin-metMbCN upon irradiating 4-H then leads to d arising from γ_2-CH_3. While multispin effects will undermine the simple r^{-6} dependence of interproton NOEs,[22] we find a semiquantitative agreement between the relative distances and NOEs (column 1 of Table I) if a is assigned to γ_1-CH and h to γ_1-CH′ (see also relaxation data). The NOEs to peak x and n are consistent with x originating from the β-CH and n from the more distant α-CH. The second and third columns in Table II show similar quantitative correlation between distance and NOEs which confirm the assignments determined above.

Dipolar Relaxation and Solution Orientation. The results of an inversion–recovery T_1 determination for the resolved Ile-99 and two heme methyl peaks are exhibited in Figure 5. The semilogarithmic plots are clearly linear for T_1, but exhibit curvature in the direction of apparent slower relaxation at long delay times. This behavior has been predicted[35] and observed[36] for protons experiencing cross-relaxation with slower relaxing protons. The initial slope of such a plot, however, is known to yield the essentially paramagnetic T_1 for the resonance. A plot similar to those in Figure 5 could not be obtained for peak h (γ_1-CH′) due to severe overlap and an ill-defined base line on the rising shoulder of the diamagnetic envelope. A good estimate of T_1 (h), however,

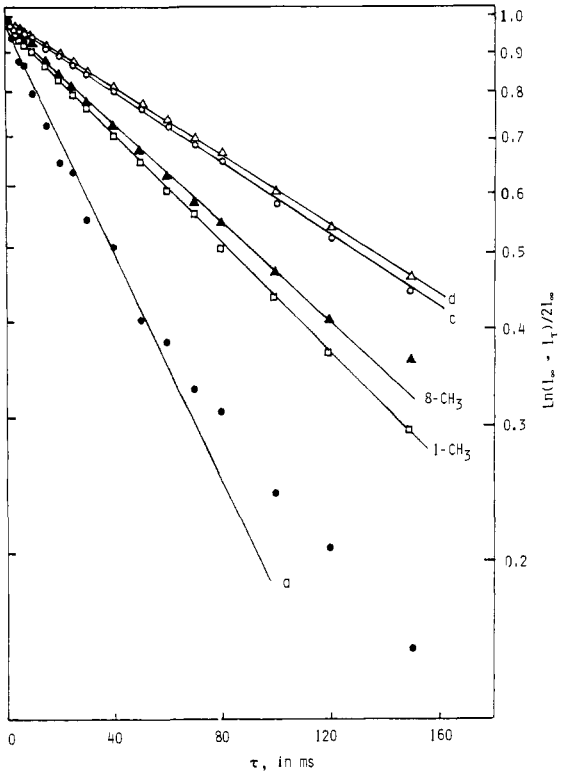

Figure 5. Plot of ln $(I_\infty - I_\tau)/(2I_\infty)$ vs. delay time, τ, for a 180°–τ–90° inversion–recovery T_1 determination for peak a (●), c (○), d (△), 1-CH_3 (□), and 8-CH_3 (▲) at 20 °C in ^2H_2O, pH 8.6. The solid lines represent the initial slopes which directly yield the T_1 values listed in Table II.

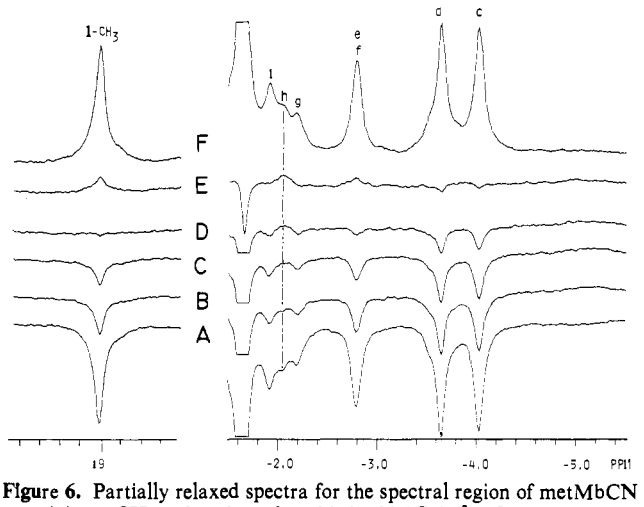

Figure 6. Partially relaxed spectra for the spectral region of metMbCN containing 1-CH_3 and peaks c, d, and h (at 20 °C, in ^2H_2O, pH 8.6). The delay time, τ, in the 180°–τ–90° inversion–recovery pulse sequence are (A) 0.5, (B) 40, (C) 50, (D) 70, and (E) 90 ms and (F) 2 s. The null point for 1-CH_3 at 19 ppm occurs at ~70 ms while that for peak h is estimated to occur at ~50 ms.

could be obtained from the relative null points of the partially relaxed spectra, as shown in Figure 6. The τ_{null} for h occurs at ~50 ms while that for the resolved 1-CH_3 signal is seen at 70 ms. Estimating T_1(h) from the relation $T_1(h) = T_1(CH_3)\tau_{null}(h)/\tau_{null}(CH_3)$ yields T_1(h) ~ 90 ms. Not even qualitative estimates of T_1s for peaks n and x are possible at this time.

The necessarily dipolar relaxation that determines T_1s for a noncoordinated residue requires for two nonequivalent protons that[18,37]

$$r_i/r_j = [T_{1i}/T_{1j}]^{1/6} \quad (2)$$

(34) This is based on the observation that even for an internally immobile pair of protons, the protein rotational correlation time of 10 ns (Johnson, R. D. Ph.D. Thesis, University of California, Davis, 1983) demands[16,19] the protons be separated by <1.9 Å; hence they must arise from a single methylene group.

(35) Granot, J. *J. Magn. Reson.* **1982**, *49*, 257.

(36) Sletten, E.; Jackson, J. T.; Burns, P. D.; La Mar, G. N. *J. Magn. Reson.* **1983**, *52*, 492.

(37) Swift, T. J. In "NMR of Paramagnetic Molecules"; La Mar, G. N., Horrocks, W. D., Holm., Eds.; Academic Press: New York, 1973; pp 53–83.

Table III. Analysis of Ile-99 Dipolar Shifts on the Basis of Axial Magnetic Anisotropy

peak	$(\Delta H/H)_{obsd}$[a]	$\Delta(\Delta H/H)_{dip}$[b]	rel[c] $\Delta(\Delta H/H)_{dip}$	$(3\cos^2\theta - 1)/r^{3}$[d]	rel[e] $(3\cos^2\theta - 1)r^{-3}$
heme 1-CH_3	+18.9	*f*		−4.00	1.76
a (γ_1-CH)	−9.31	4.03	1.00	−2.27	1.00
h (γ_1-CH′)	−2.2	1.09	0.27	+1.60	−0.70
c (δ-CH)	−4.03	1.53	0.38	−2.60	1.14
d (γ_2-CH_3)	−3.55	1.38	0.34	−2.23	0.98
n (α-CH)	−0.21	*g*		+0.65	
x (β-CH)	−0.08	*g*		+0.13	

[a] Shifts in ppm, relative to DSS, in H_2O solution at 25 °C. [b] Difference in observed shift (solely dipolar for Ile-99) between 50 and 5 °C, in ppm. [c] Relative ratio of difference between 50° and 5° shifts, with that for peak a (γ_1-CH) normalized to unity. [d] Axial geometric factor calculated from X-ray coordinates as described in the Experimental Section, in 10^{21} cm^{-3}. [e] Relative values of axial geometric factor with that for peak a normalized to unity. [f] The observed shift contains large scalar contribution. [g] Not resolved over sufficient temperature range to yield data.

The T_1s for 8-CH_3 (the heme methyl peak with negligible non-metal dipolar contribution[38] to T_1 relaxation), a, c, and d, are taken from the initial slopes of Figure 5 and are also listed in the first column of Table II. In the second column, we list the iron–proton distances (r_i) averaged over such internal motion as methyl rotation, as determined from the X-ray coordinates for the crystal structure of metMbH_2O, deoxyMb, and MbO_2. A refined structure for the protein form of current interest, metMbCN, is not available at this time. In the last column of Table II we list the range of r_i values obtained from differential relaxation using eq 2 and the known heme methyl iron distance, $r(CH_3) = \langle r^3(CH_3)\rangle^{1/3} = 6.10$ Å.[39]

Several conclusions can be reached upon inspecting Table II. One is that the closest proton to the iron is indeed γ_1-CH, as deduced from NOE data above, and another is that there is generally a very good correlation between the solution-determined distances and the range found in the various crystals. The only discrepancy outside of the apparent range of values is that we find γ_1-CH at least 0.4 Å further from the iron than found in any of the X-ray structures.[7,8] Thus we can conclude that the orientation of Ile-99 FG5 relative to the heme is essentially the same in solution and in crystals. There are small systematic differences in r_i as obtained from X-ray structures.[7,8] Thus metMbH_2O has δ-CH_3 7.1 Å and γ_2-CH_3 6.5 Å from the iron, while deoxyMb and MbO_2 have the two methyls comparably close (6.6, 6.5 Å). Since metMbH_2O also has γ_1-CH slightly further away, it appears that different crystal structures reflect small differences in the rotational angle about the C_β–C_{γ_1} bond, consistent with a minor amount of mobility for the extreme end of the side chain.

Side Chain Mobility. The interproton distance for the γ-geminal protons (1.77 Å) allows the time development of the NOE in Figure 4 to be analyzed via the eq 3, where ρ_h is the intrinsic

$$\eta_h(t) = (\sigma_{ha}/\rho_h)(1 - e^{-\rho_h t}) \qquad (3)$$

spin–lattice relaxation rate for spin h and σ_{ha} is the cross-relaxation rate between spin h and a.[24,25,31] Analysis of the data yields the fit represented by the solid line through the points for peak h in Figure 4, which yields $\sigma_{ha} = -15.5 \pm 1.5$ s^{-1}. The correlation time, τ_i, responsible for the cross-relaxation at high magnetic field strength ($\omega^2\tau^2 \gg 1$) is given by[25] eq 4 ($r = 1.77$ Å), yielding $\tau_i = 8.5 \pm 1.0$ ns.

$$\sigma_{ha} = -\frac{\hbar^2\gamma_H^2}{10 r_{ha}^6}\,\tau_i \qquad (4)$$

The rotational correlation time originates from overall protein tumbling and internal motion of the interproton vector. The tumbling time for myoglobin at low concentrations has been determined by several methods, including ^2H quadrupolar relaxation (11 ns),[34] γ–γ correlation (10 ns),[40] and natural abundance ^{13}C α-carbon relaxation (10–13 ns, depending on choice of the r_{CH} value), with the latter two results translated to 25 °C in the usual way by temperature corrections.[40] Taking a value of 11 ± 2 ns for the tumbling time, we see that this is only marginally different from the value of 8.5 ns for the methylene rotational correlation time. The internal mobility of the Ile γ_1 methylene will be affected by rotations about the α–β and β–γ_1 bonds, and the relevant motional model for these rotations will be restricted diffusion, with bond rotations of a certain angular range.[43,44] Wittebort et al.[45] have examined the internal mobility of seven of the nine Ile γ_1 carbons of myoglobin by natural-abundance ^{13}C NMR (exclusive of Ile-99), and report that helical back-bone restrictions confine rotations about α–β to less than ±20°, which is too small a range to be measurable by NMR relaxation. Analysis of the Ile-99 methylene pair cross-relaxation rate in terms of β–γ rotations yields an angular range of ±30° (uncertain by ±12°). While we see oscillatory mobility for Ile-99 in myoglobin, this result is quite different from the motional behavior observed for Ile-98 in lysozyme,[24] where β–γ_1 rotational mobility was calculated to be ±57° if α–β rotation was neglected. The small degree of mobility for Ile-99 is in agreement with the previous ^{13}C NMR results for different isoleucines in myoglobin, two having angular ranges about β–γ_1 less than ±20°, the remaining five with ranges from ±30° to ±50°.[45]

The Nature of Magnetic Anisotropy. While ESR spectra have yielded rhombically anisotropic *g* values of both low-spin ferric porphyrin complexes[46] and metcyanohemoproteins,[47] the ^1H NMR of the models clearly show that this anisotropy is not present in solution at ambient temperature.[20] The qualitative analysis of the hyperfine-shifted peaks of metcyanohemoproteins requires the knowledge of the magnetic susceptibility tensor and the location of the magnetic axes relative to the porphyrin coordinate system.[19,48] With these data, side chain dipolar shifts would provide qualitative information on the structure of the heme pocket via eq 1. Our data show clearly that axial anisotropy is insufficient to account for the observed Ile-99 dipolar shifts. The dipolar shifts require knowledge of the diamagnetic resonance position. However, for the present, it is sufficient to note that the relative dipolar shifts for nonequivalent protons are proportional to their slopes in the Curie plot in Figure 3. Such data are given, $(\Delta(\Delta H/H)_{dip})$, for the resolved peaks in the second and third columns of Table III. With only axial anisotropy, the relation[18,37]

$$(\Delta H/H)^i_{dip}/(\Delta H/H)^j_{dip} = (3\cos^2\theta_i - 1)r_i^{-3}/[(3\cos^2\theta_j - 1)r_j^{-3}] \qquad (5)$$

must hold. The calculated axial geometry factors and their relative values are listed in column 4 and 5 of Table III, which clearly

(38) Unger, S. B.; La Mar, G. N., unpublished results.
(39) Accurate determination of the distance by averaging over rotation yields a value 6.10 Å, which is slightly shorter than that used previously.[18,21]

(40) Marshall, A. G.; Lee, K. M.; Martin, P. W. *J. Am. Chem. Soc.* **1980**, *102*, 1460.
(41) Gilman, J. *Biochemistry* **1979**, *18*, 2273.
(42) Dill, K.; Allerhand, A. *J. Am. Chem. Soc.* **1979**, *101*, 4376.
(43) London, R. E.; Avitabile, J. *J. Am. Chem. Soc.* **1978**, *100*, 7159.
(44) Wittebort, R. J.; Szabo, A. *J. Chem. Phys.* **1977**, *69*, 1722.
(45) Wittebort, R. J.; Rothgeb, T. M.; Szabo, A.; Gurd, F. R. N. *Proc. Natl. Acad. Sci. U.S.A.* **1979**, *76*, 1059.
(46) Chacko, V. P.; La Mar, G. N. *J. Am. Chem. Soc.* **1982**, *104*, 7002.
(47) Hori, H. *Biochim. Biophys. Acta* **1971**, *251*, 227.
(48) Shulman, R. G.; Glarum, S. H.; Karplus, M. *J. Mol. Biol.* **1971**, *57*, 93.

show that the dipolar shifts are inconsistent with only axial anisotropy. Thus eq 5 predicts shifts in opposite direction for δ-CH_3 and γ_2-CH_3, although comparable shifts in the same direction are observed. The pattern of dipolar shifts require a substantial rhombic anisotropy. The orientation of the g tensor and the g values obtained by Hori[47] for metMbCN at 20 K fail to account qualitatively for the observed pattern, suggesting that the magnetic axes differ at 20 and 298 K. This is not surprising since variable-temperature ESR has demonstrated that the magnetic axes change with temperature for two related Mb derivatives.[49,50] While the observed dipolar shifts can, in principle, provide both the components of the susceptibility tensor as well as the location of the magnetic axes, for such an analysis to be meaningful, it is necessary to assign unambiguously other amino acid side chains that exhibit sizable dipolar shifts and whose orientation can be ascertained from relaxation data.

It may be noted that the large upfield dipolar shift for γ_1-CH dictactes that the rhombic axes are aligned approximately so as to cause upfield dipolar shifts for pyrrole II and IV on which are appended 3-CH_3 and 8-CH_3. The nature of the rhombic geometric factor thus requires that the rhombic dipolar shift be negative (downfield) in the region of pyrrole I and III on which are located 1-CH_3 and 5-CH_3. Thus even the well-characterized asymmetry of the heme methyl hyperfine shifts, which have been generally interpreted[12,48,51] in terms of a completely scalar or contact interaction involving the raising of the orbital degeneracy of the porphyrin e_3 π orbitals, may have significant contribution from rhombic dipolar shifts.

Studies aimed at effecting sufficient unambiguous assignments of other purely dipolar-shifted amino acid side chain signals to determine the susceptibility tensor are in progress in this laboratory.

Acknowledgment. We thank Dr. J. Lecomte for expert assistance with the protein coordinate calculations and are grateful for the cooperation and assistance provided by the University of California, Davis Nuclear Magnetic Resonance Facility, and the Computer Graphics Laboratory at the Unversity of California, San Francisco. This work was supported by grants from the National Science Foundation, CHE-81-08766, and in part, from the National Institutes of Health, HL-16087.

Reglstry No. Ile, 73-32-5; iron, 7439-89-6.

(49) Hori, H.; Ikeda-Saito, M.; Yonetani, T. *Nature (London)* **1980**, *288*, 501.
(50) Hori, H.; Ikeda-Saito, M.; Yonetani, T. *J. Biol. Chem.* **1982**, *257*, 3636.
(51) Traylor, T. G.; Berzinis, A. P. *J. Am. Chem. Soc.* **1980**, *102*, 2844.

Stereochemical Studies on the Reactions Catalyzed by the PLP-Dependent Enzyme 1-Aminocyclopropane-1-carboxylate Deaminase

Hung-wen Liu,† Richard Auchus, and Christopher T. Walsh*

Contribution from the Department of Chemistry, Massachusetts Institute of Technology, Cambridge, Massachusetts 02139. *Received November 7, 1983*

Abstract: The stereochemical course of 1-aminocyclopropane-1-carboxylate deaminase which catalyzes the fragmentation of the cyclopropane substrate to α-ketobutyrate and ammonia has been unraveled with the help of substrates stereospecifically labeled with deuterium and/or tritium, and this has afforded important information about the process occurring at the active site during enzymatic conversion. These results can be summarized as follows: (1) ring cleavage is regiospecific and only occurs between the *pro-S* and the α-carbon of ACPC; (2) β-H abstraction is *pro-R* stereospecific and the reprotonation at β-C is mediated by the same enzyme base which is partially shielded and located at the *si* face relative to α-C; (3) preferred conformation of the β,γ-olefinic PLP-*p*-quinoid α-anion complex is cisoid and the geometry of the terminal double bond, if trisubstituted, favors *E*, while the major conformation of the nascent intermediate, aminocrotonate, is *Z* (defined as relative to the amino group); (4) protonation at C-4 is mediated by a different enzyme base which is not shielded and is situated at the *si* face with respect to α-C.

The unusual cyclopropanoid amino acid 1-aminocyclopropane 1-carboxylic acid (ACPC) is a natural product found in many plants.[1] Recent studies had implicated it as a precursor of ethylene, a fruit-ripening and growth-regulating plant hormone.[2] The mechanism of this physiologically significant and commercially important fragmentation process is as yet unknown but under examination.[3]

ACPC is formed biosynthetically from methionine presumably via *S*-adenosylmethionine catalyzed by a pyridoxal 5′-phosphate (PLP) linked enzyme (ACPC synthase) which appears to carry out a formal internal γ-displacement reaction initiated by an α-anion equivalent. An alternate route for biological breakdown of ACPC, besides the plant-mediated fragmentation to ethylene, is a cleavage reaction producing α-ketobutyrate **2** and ammonia carried out by certain bacteria. Pseudomonads which can grow on ACPC as sole nitrogen source have been isolated. From these bacteria the PLP-containing enzyme ACPC deaminase, mediating the reaction delineated by eq 1, has been purified to homogeneity.[4] This enzyme will also catalyze the ring-opening process of 2-

† Present address: Department of Chemistry, University of Minnesota, Minneapolis, MN 55455.

(1) (a) Burroughs, L. F. *Nature* **1957**, *179*, 360. (b) Vahatalo, M. L.; Virtanen, A. I. *Acta Chem. Scand.* **1957**, *11*, 741.
(2) (a) Adams, D. O.; Yang, S. F. *Proc. Natl. Acad. Sci. U.S.A.* **1979**, *76*, 170. (b) Lussen, K.; Naumann, K.; Schroder, R. *Z. Pflanzenphysiol.* **1979**, *92*, 285. (c) Konze, J. R.; Kende, H. *Planta* **1979**, *146*, 293.
(3) (a) Yang, S. F.; Adams, D. O. "The Biochemistry of Plants"; Stumpf, P. K., Ed.; Academic Press: New York, 1980; Vol. 4, pp 163 ff. (b) Adlington, R. M.; Aplin, R. T.; Baldwin, J. E.; Rawlings, B. J.; Osborne, D. *J. Chem. Soc., Chem. Commun.* **1982**, 1086. (c) Adlington, R. M.; Baldwin, J. E.; Rawlings, B. J. *Ibid.* **1983**, 290. (d) Pirrung, M. C. *J. Am. Chem. Soc.* **1983**, *105*, 7207. (e) Peiser, G. D.; Wang, T. T.; Hoffman, N. E.; Yang, S. F.; Liu, H. W.; Walsh, C. T. *Proc. Natl. Acad. Sci. U.S.A.* **1984**, *81*, 3059.
(4) Honma, M.; Shimomura, T. *Agric. Biol. Chem.* **1978**, *42*, 1825.

0002-7863/84/1506-5335$01.50/0